Materials Research Bulletin 48 (2013) 146–150

Contents lists available at SciVerse ScienceDirect

Materials Research Bulletin

journal homepage: www.elsevier.com/locate/matresbu

Triazoloisoquinoline-based dual functional dyestuff for dye-sensitized solar cells

Che-Lung Lee [a], Wen-Hsi Lee [a], Cheng-Hsien Yang [b,*], Hao-Hsun Yang [b], Jia-Yaw Chang [c,*]

[a] Department of Electrical Engineering, Nation Cheng Kung University, No. 1, Daxue Rd., East Dist., Tainan City 70101, Taiwan, ROC
[b] ShiFeng Technology Co., Ltd. Rm. 410, Bldg. R2, No. 31, Gongye 2nd Rd., Annan District, Tainan, 70955, Taiwan, ROC
[c] Department of Chemical Engineering, Nation Taiwan University of Science and Technology, No. 43, Sec. 4, Keelung Rd., Da'an Dist., Taipei City 106, Taiwan, ROC

ARTICLE INFO

Article history:
Received 23 May 2012
Received in revised form 5 October 2012
Accepted 15 October 2012
Available online 23 October 2012

Keywords:
A. Thin films
B. Chemical synthesis
C. Nuclear magnetic resonance
D. Electrical properties

ABSTRACT

Triazoloisoquinoline contains electron-rich nitrogen and oxygen heteroatoms in a heterocyclic structure with high electron-donating ability. By utilizing this feature, two organic dyesutffs containing triazoloisoquinoline were synthesized and used in the fabrication of dye-sensitized solar cells (DSSCs), overcoming the deficiency of ruthenium dyestuff absorption in the blue part of the visible spectrum. This method also fills the blanks of ruthenium dyestuff sensitized TiO_2 film, and forms a compact insulating molecular layer due to the nature of small molecular organic dyestuffs. The incident photon-to-electron conversion efficiency of N719 at shorter wavelength regions is 35%. After addition of triazoloisoquinoline-based dyestuff for co-sensitization, the IPCE at 350–500 nm increased significantly. This can be attributed to the increased photocurrent of the cells, which improves the dye-sensitized photoelectric conversion efficiency from 4.49% to 5.15%, which the overall conversion efficiency increased by about 15%. As a consequence, this low molecular weight organic dyestuff is a promising candidate as co-adsorbent and co-sensitizer for highly efficient dye-sensitized solar cells.

1. Introduction

Dye-sensitized solar cells (DSSCs) have attracted much scientific attention in recent years because of their low cost, relatively high photoelectric conversion efficiency (11%) and simple fabrication process [1–4]. However, it is necessary to further improve the energy conversion efficiency of DSSCs for successful commercialization. Many studies have focused on the broadening of the absorption spectra of the cells, including tandem DSSCs, hybrid DSSCs and co-sensitized DSSCs [5–8]. The cost of the multilayered photoelectrode process is high for the fabrication of tandem and hybrid DSSCs. However, co-sensitized DSSCs have attracted much attention because of the easy dying process.

In the literature, most reports of co-sensitized DSSCs focus on the extension of solar absorption spectra from the visible to the near-infrared (NIR) region [6,9,10]. For example, Yum et al. fabricated a solar cell based on co-sensitization of 3-{5′-[*N*,*N*-bis(9,9-dimethylfluorene-2-yl)phenyl]-2,2′-bisthiophene-5-yl}-2-cyanoacrylic acid (JK2) and 5-carboxy-2-[[3-[(1,3-dihydro-3,3-dimethyl-1-ethyl-2H-indol-2-ylidene)methyl]-2-hydroxy-4-oxo-2-cyclobuten-1-ylidene]methyl]-3,3-trimethyl-1-octyl-3H-indolium (SQ1) [6] By using the concept of two complementary organic dyestuffs, they achieved higher efficiency-7.36% than that seen with a single dye device. Using this concept and a multilayered photoanode, Miao et al. obtained a high efficiency of 11.05% by choosing (tri(isothiocyanato)(2,2′:6′,2″-terpyridyl-4,4′,4″-tricarboxylic acid)ruthenium(II)) (BD) to overcome the deficient areas in the NIR absorption spectra of *cis*-dithiocyanate-*N*,*N*′-bis-(4-carboxylate-4-tetrabutyl ammoniumcarboxylate-2,2′-bipyridine)ruthenium(II) (N719) [9] However, to the best of our knowledge, few studies focus on the use of co-sensitization to broaden the light absorption spectra of N719 in the blue part of the visible spectrum. In this work we report the synthesis of the organic dyestuff triazoloisoquinoline **5**, which can be used as a co-adsorbent to modify the monolayer of a N719 dying-TiO_2 photoanode and co-sensitized dyestuff to absorb in the blue part of the visible spectrum. By combining the triazoloisoquinoline **5** and the N719 sensitizers, greater higher efficiency is obtained than seen with the individual dye cells.

2. Experimental

2.1. General information and materials

Scheme 1 outlines how the dyestuff was synthesized. All starting materials were purchased from Aldrich and TCI, and were used without further purification. N719, titania pastes (Ti-Nanoxide T series) and transparent conducting oxide (TCO,

---

* Corresponding authors.
E-mail addresses: chelung168@gmail.com (C.-L. Lee), jasonyang@fusol-material.com (C.-H. Yang), jychang@mail.ntust.edu.tw (J.-Y. Chang).

0025-5408/$ – see front matter © 2012 Elsevier Ltd. All rights reserved.
http://dx.doi.org/10.1016/j.materresbull.2012.10.025

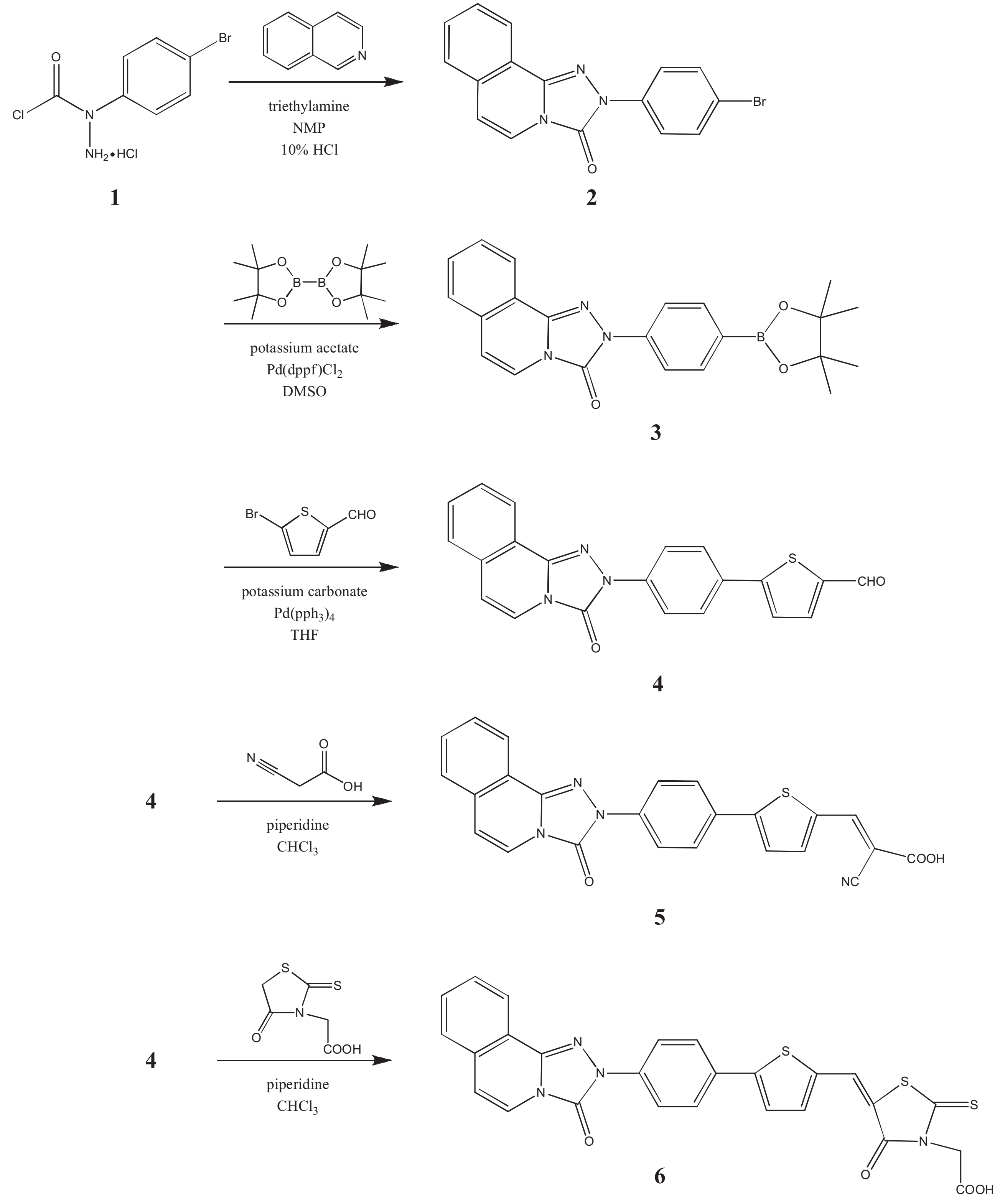

Scheme 1. Synthesis of organic dyestuffs **5** and **6**.

F-doped SnO_2, 10 Ω square^{-1}) were purchased from Solaronix SA. With regard to the electrolyte, 0.6 M propylmethylimidazolium iodide ([PMI][I]) + 0.1 M lithium iodide (LiI) + 0.03 M iodine (I_2) + 0.5 M 4-tert-butylpyridine (TBP) in 3-methoxypropionitrile (MPN) was used in this work. The UV–vis spectra were measured in DMF solution on an Agilent 8453 spectrophotometer. ^{1}H NMR and ^{13}C NMR spectra were measured in d_6-DMSO solution on a Bruker Avance-300 (300 MHz) NMR spectrometers with tetramethylsilane (TMS) as the internal standard. The EI-Mass spectra were recorded on a Bruker APEX II.

*2.2. Synthesis of 2-(4-bromophenyl)-[1,2,4]triazolo[3,4-a]isoquinolin-3(2H)-one (**2**)*

A three-neck flask was charged with α-chloroformyl p-bromophenyl hydrazine hydrochloride (5.3 g, 18.5 mmol). This was dissolved in 50 ml of N-methyl pyrrolidinone (NMP) with stirring. Triethylamine (2.8 ml, 27.7 mmol) was then added dropwise into the mixture at room temperature. The mixture was heated at 80 °C for 16 h. Then, after adding 10% hydrochloric acid, the mixture was filtered to obtain a crude product. This crude product was purified by recrystallization technique (EtOAc-Toluene) to get compound **2**: yellow crystals; yield 4.2 g (66.7%); ^{1}H NMR (300 MHz, d_6-DMSO): δ 8.28 (d, 1H, *J* = 7.65 Hz), 8.08 (d, 2H, *J* = 8.81 Hz), 7.83 (d, 1H, *J* = 7.65 Hz), 7.77–7.66 (m, 5H), 7.03 (d, 1H, *J* = 7.44 Hz).

*2.3. Synthesis of 2-(4-(4,4,5,5-tetramethyl-1,3,2-dioxaborolan-2-yl)phenyl)-[1,2,4] triazolo [3,4-a]isoquinolin-3(2H)-one (**3**)*

In a round-bottom flask, compound **2** (5.6 g, 16.3 mmol), 4,4,5,5-tetramethyl-2-(4,4,5,5-tetramethyl-1,3,2-dioxaborolan-2-yl)-1,3,2-dioxaborolane (4.4 g, 17.1 mmol) and potassium acetate (4.8 g, 49.0 mmol) were dissolved in dimethyl sulfoxide (DMSO) under nitrogen atmosphere. After adding a catalyst of dichloro-[1,1′-bis(diphenylphosphino)ferrocenyl]palladium(II) (Pd(dppf)Cl_2), the mixed solution was heated at 80 °C for 6 h with vigorous stirring. It was then poured into EtOAc-water for extraction. The organic phase was concentrated and adsorbed on silica gel and purified by column chromatography using hexane/EtOAc mixture (5:1) as the eluant: white powder; yield 5.32 g (84.2%); ^{1}H NMR (300 MHz, d_6-DMSO): δ 8.31 (d, 1H, *J* = 7.53 Hz), 8.17 (d, 2H, *J* = 8.23 Hz), 7.84 (d, 3H, *J* = 8.57 Hz), 7.77–7.66 (m, 3H), 7.02 (d, 1H, *J* = 7.44 Hz), 1.32 (s, 12H).

*2.4. Synthesis of 5-(4-(3-oxo-[1,2,4]triazolo[3,4-a]isoquinolin-2(3H)-yl)phenyl) thiophene- 2-carbaldehyde (**4**)*

In a three-necked round-bottomed flask (25 mL) equipped with a reflux condenser, compound 3 (1.71 g, 4.4 mmol), 5-bromothiophene-2-carbaldehyde (1.0 g, 5.2 mmol), and 2 M potassium carbonate solution were added to a suspension of Pd(PPh_3)$_4$ (3.0 mol%) in tetrahydrofuran (30 mL) at ambient temperature under nitrogen. The reaction mixture was heated to 80 °C with rapid stirring for 16 h. After cooling, the resulting solution was poured into water. The separated solid was filtered and thoroughly washed with water–acetone and dried: pale yellow powder; yield 1.0 g (61.6%); ^{1}H NMR (300 MHz, d_6-DMSO): δ 9.23 (s, 1H), 8.32 (d, 1H, *J* = 7.56 Hz), 8.24 (d, 2H, *J* = 8.53 Hz), 8.07 (d, 1H, *J* = 3.81 Hz), 8.01 (d, 2H, *J* = 8.60 Hz), 7.86–7.67 (m, 5H), 7.04 (d, 1H, *J* = 7.39 Hz).

*2.5. Synthesis of 2-cyano-3-(5-(4-(3-oxo-[1,2,4]triazolo[3,4-a]isoquinolin-2(3H)-yl) -phenyl) thiophen-2-yl)acrylic acid (**5**)*

In a three-neck bottle, compound **4** (1.2 g, 3.3 mmol), 2-cyanoacetic acid (0.6 g, 6.5 mmol) and piperidine (0.08 g, 0.98 mmol) were dissolved in chloroform. The mixed solution was refluxed for 16 h with rapid stirring. After cooling, the resulting solution was poured into EtOAc-MeOH. The separated solid was filtered and thoroughly washed with EtOAc and MeOH and dried: pale orange powder; yield 1.2 g (85.0%); ^{1}H NMR (300 MHz, d_6-DMSO): δ 8.32 (d, 1H, *J* = 7.50 Hz), 8.23 (s, 1H), 8.20 (d, 2H, *J* = 3.20 Hz), 7.93 (d, 2H, *J* = 8.72 Hz), 7.89–7.67 (m, 6H), 7.03 (d, 1H, *J* = 7.46 Hz); ESI-MS *m*/*z* 437 ($M-H^+$).

*2.6. Synthesis of 2-(5-(4-(3-oxo-[1,2,4]triazolo[3,4-a]isoquinolin-2(3H)-yl)phenyl) thiophen-2-yl) methylene)-4-oxo-2-thioxothiazolidin-3-yl)acetic acid (**6**)*

In a three-neck bottle, compound **4** (1.2 g, 3.3 mmol), 2-(4-oxo-2-thioxothiazolidin-3-yl) acetic acid (rhodanine-3-acetic acid) (0.7 g, 3.8 mmol) and piperidine (0.05 g, 0.57 mmol) were dissolved in chloroform. The mixed solution was refluxed for 24 h with rapid stirring. After cooling, the resulting solution was poured into EtOAc-MeOH. The separated solid was filtered and thoroughly washed with EtOAc and MeOH and dried: reddish-orange powder; yield 0.98 g (95.4%); ^{1}H NMR (300 MHz, d_6-DMSO): δ 8.32 (d, 1H, *J* = 7.60 Hz), 8.22 (d, 2H, *J* = 8.75 Hz), 8.21 (s, 1H), 8.01–7.95 (m, 2H), 7.85–7.67 (m, 6H), 7.04 (d, 2H, *J* = 7.47 Hz), 4.66 (s, 2H); ESI-MS *m*/*z* 543 ($M-H^+$).

3. Fabrication of photovoltaic devices

Eight micrometer nanocrystalline TiO_2 photoelectrodes were prepared from a titania paste (Ti-Nanoxide T series, Solaronix SA). The paste was applied to a transparent conducting oxide by doctor-blading techniques and annealed at 450 °C for 30 min in air. The thickness of the TiO_2 films was measured with an Alpha-Step 300 profiler. When the TiO_2 electrodes cooled down to around 100 °C, the electrodes were dipped in dye solutions, which included 0.5 mM N719 and different concentrations of dyestuffs **5** or **6** in tert-butanol/acetonitrile (AN) (1:1 in volume) (device A: N719: dyestuff **5** (1:0); device B: N719: dyestuff **5** (1:1); device C: N719: dyestuff **5** (1:0.25); device D: N719: Dyestuff **5** (0:1)). The TiO_2 electrodes were immersed in the dye solutions and then kept at 25 °C for more than 12 h to allow the dye to adsorb to the TiO_2 surface, and rinsed with the same solvents. The dye-loaded TiO_2 film as the working electrode and Pt-coated TCO (about 20 nm) as the counter electrode were separated by a hot-melt Surlyn sheet (60 μm) and sealed together by pressing them under heat. The electrolytes were introduced into the gap between the working and the counter electrodes from two holes predrilled on the back of the counter electrode. Finally, the two holes were sealed with a Surlyn film covering a thin glass slide under heat.

4. Photovoltaic measurement

The current density–voltage (*J*–*V*) characteristics in the dark and under illumination were measured with a Keithley 2400 sourcemeter. The photocurrent was measured in a nitrogen-filled glove box under a solar simulator (Oriel 96000 150W) with AM 1.5G-filtered illumination (100 mW cm^{-2}). The spectra-mismatch factor of the simulated solar irradiation was corrected using an Schott visible-color glass-filtered (KG5 color filter) Si diode (Hamamatsu S1133) [11]. The active area of the device was 0.25 cm^2.

5. Results and discussion

Co-adsorbents and co-sensitizers have both been extensively studied in DSSCs. However, to the best of our knowledge, few reports discuss the relationship between the two. Triazoloisoquinoline contains electron-rich nitrogen and oxygen heteroatoms in a heterocyclic structure with high electron-donating ability. This study is the first report of using triazoloisoquinoline dyestuffs as a co-adsorbent to modify the monolayer of a N719 dying-TiO_2 photoanode and co-sensitizer to absorb the blue part of the visible spectrum. The synthetic routes of organic dyestuffs **5** and **6** are depicted in Scheme 1. They consist of treatment of triazoloisoquinolines substituted tetramethyl-dioxaborolane with 5-formyl-2bromothiophene under conditions for Suzuki coupling, followed

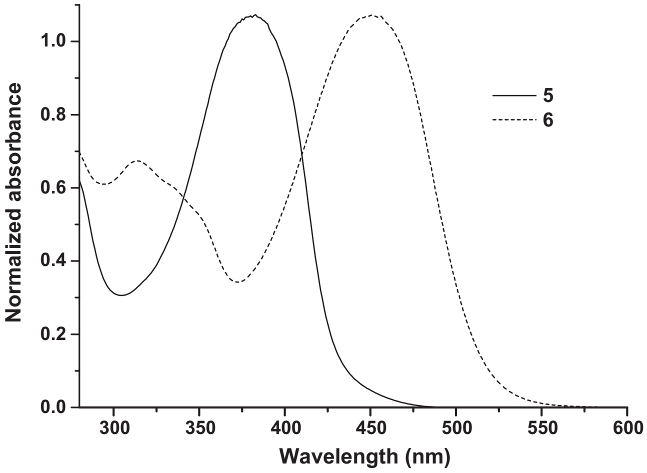

Fig. 1. Normalized UV–vis spectra of dyestuffs **5** and **6** in DMF.

by condensation with cyanoacrylic acid or rhodanine-3-acetic acid in the presence of piperidine.

The absorption spectra of the dyestuffs in DMF solutions are shown in Fig. 1, and the corresponding data are presented in Table 1. The absorption spectra show two major bands at ca. 250–350 nm and at ca. 350–600 nm. UV absorption is attributed to localized aromatic π–π^* transitions. In the visible region, this may be attributed to intramolecular charge transfer (ICT) absorption, because an efficient charge-separated excited state could be produced between the triazoloisoquinoline and the cyanoacrylic/rhodanine-3-acetic acid moieties [12]. As shown in Table 1, the ICT absorption (λ_{max}) appeared at 380 nm for **5**, and 451 nm for **6**. The molar extinction coefficients in the visible region were 29,651 $M^{-1}\,cm^{-1}$ for **5**, and 29,353 $M^{-1}\,cm^{-1}$ for **6**, and all of these are twice as high as those of the ruthenium complexes [13]. Compound **6** with rhodanine-3-acetic acid as the acceptor shows a significant bathochromic shift in the S_0–S_1 absorption band compared with that of compound **5**. This red-shift may favor light harvesting and hence photocurrent generation in DSSCs. Therefore, a simple cell was fabricated (FTO/8 μm TiO_2/MPN electrolyte/Pt) for verification this concept. All the essential properties of these DSSC dyestuffs are listed in Table 1. Under the standard AM 1.5G irradiation, the maximum efficiency (η (%)) for compound **5** with an active cell area of 0.25 cm^2 was calculated to be 1.2%, while the cell based on compound **6** showed a relatively low short-circuit current (J_{sc}) and open-circuit voltage (V_{oc}), leading to a lower η value of 0.54%. This result indicates that rhodanine-3-acetic acid is a poor anchor in comparison to cyanoacrylic acid. These results agree with the experimental data in Liang et al. and Tian et al. [14,15]. However, it is necessary to consider the efficiency of co-sensitizer, and also compound **6** based on rhodanine-3-acetic acid is excluded from the follow-up experiments.

Table 1
Optical and DSSC performance parameters of dyestuffs **5** and **6**.

Dyestuff	λ_{max}/nm[a] (ε/$M^{-1}\,cm^{-1}$)	J_{sc} ($mA\,cm^{-2}$)	V_{oc} (V)	FF	η (%)[b]
5	277 (19435), 380 (29651)	2.95	0.56	0.68	1.12
6	314 (19115), 451 (29353)	1.96	0.50	0.55	0.54

[a] Absorption spectra were measured in DMF.

[b] Performances of DSSCs were measured with 0.25 cm^2 working area and the photoanodes were dyed with DMF solution.

Table 2
Photovoltaic parameters of the DSSCs with N719: dyestuff **5** sensitizers in different molar ratios under AM 1.5G sunlight.[a]

	Dyestuffs molar ratio	J_{sc} ($mA\,cm^{-2}$)	V_{oc} (V)	FF	η (%)
Device A	N719	9.36	0.72	0.67	4.49
Device B	N719-Dyestuff **5** 1:1	9.66	0.67	0.66	4.31
Device C	N719-Dyestuff **5** 1:0.25	10.68	0.70	0.69	5.15
Device D	Dyestuff **5**	3.25	0.58	0.61	1.14

[a] Performances of DSSCs were measured with 0.25 cm^2 working area.

In order to clarify the role played by the triazoloisoquinoline dyestuff in the DSSCs, different molar ratios of cosensitizers based on N719 and dyestuff **5** were designed. All the essential properties of these cells are listed in Table 2, and the respective *J*–*V* curves are shown in Fig. 2. Under the standard AM 1.5G irradiation, the maximum efficiency (η) for the N719-sensitized solar cell-device A with an active area of 0.25 cm^2 was calculated to be 4.49%, with a J_{sc} of 9.36 $mA\,cm^{-2}$, a V_{oc} of 0.72 V and a fill factor (FF) of 0.67. However, device D, based on dyestuff **5**, showed relatively low J_{sc}-3.25 $mA\,cm^{-2}$, V_{oc}-0.58 V and FF-0.61, leading to a lower η value of 1.14%. It is reasonable that dyestuff **5** exhibits narrower absorption in the blue part of the visible region (as shown in Fig. 1) and hence could not capture enough solar radiation energy in comparison with N719. In addition, the large π-conjugated system of triazoloisoquinoline causes stronger intermolecular π–π interaction, leading to unfavorable π-stacked dye aggregation on TiO_2 in single sensitizer dying device D. Generally, close π-stacked dye aggregation leads to inefficient electron injection, resulting in a low η value due to the formation of excited triplet states [16]. Because of these physical properties, dyestuff **5** is used as the co-adsorbent and co-sensitizer for DSSCs. Interestingly, device C sensitized by N719-dyestuff **5** with 1–0.25 molar ratio produced the best results, and even better than those seen with devices A and B, with J_{sc}-10.68 $mA\,cm^{-2}$, V_{oc}-0.70 V and FF-0.69 and an overall conversion efficiency η of 5.15%. One can see from Fig. 2 and Table 2 that the V_{oc} of devices B and C were around 0.67–0.70 V by using co-sensitizers, but the J_{sc} of these devices showed excellent performance in comparison with device A, which was based on single sensitizer-N719. This result suggests that the quasi-Fermi level of the co-sensitizer dyed TiO_2 layer moves downward relative to the iodide/triiodide, which leads to a decrease in V_{oc}, but extends the absorption area of the visible

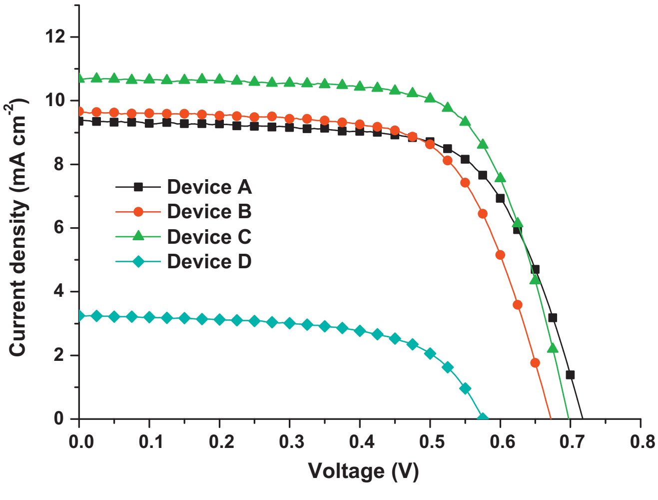

Fig. 2. *J*–*V* curves of solar cells sensitized by N719 (device A), N719: dyestuff **5** (1:1) (device B), N719: dyestuff **5** (1:0.25) (device C), and dyestuff **5** (device D) with 8.0 μm single layer nanocrystalline TiO_2 electrodes.

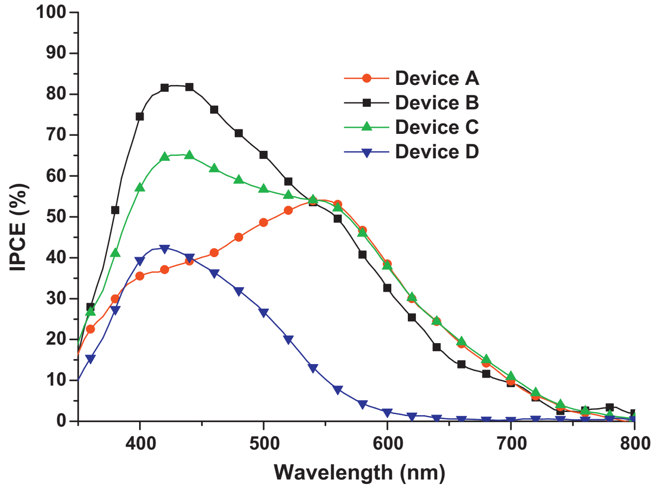

Fig. 3. IPCE action spectra of solar cells sensitized by N719 (device A), N719: dyestuff **5** (1:1) (device B), N719: dyestuff **5** (1:0.25) (device C), and dyestuff **5** (device D) with 8.0 μm single layer nanocrystalline TiO_2 electrodes.

spectrum after being co-sensitized with dyestuff **5** and N719, which enhances J_{sc}. This result is also in agreement with the observation of the incident photon-to-electron conversion efficiency (IPCE) action spectra of DSSCs presented in Fig. 3. On the other hand, device D-sensitized with dyestuff **5** exhibits a lower V_{oc}-0.58 V, while devices B and C co-sensitized with dyestuff **5** and N719 show only small changes in the V_{oc} value, to 0.67 V and 0.70 V, respectively. These values are very close to that of device A based on N719, which is 0.72 V. This result is attributed to the co-adsorbent effect of dyestuff **5**, which is applied successfully to prepare an insulating molecular layer with N719 [17,18].

IPCE as a function of wavelength was measured to evaluate the photo-response of the photoelectrodes in the whole spectra region. As shown in Fig. 3, the maximum IPCE of dyestuff **5** based device D was *ca.* 43% at 420 nm. This indicates that dyestuff **5** has good light harvesting effects at shorter wavelength regions. Device A exhibits the maximum IPCE of *ca.* 52% at 570 nm for the N719 sensitized solar cell. The incident photon-to-electron conversion efficiency of N719 at shorter wavelength regions (*ca.* 35% at 420 nm) is thus not as good as at longer wavelength owns [19]. This is a niche for organic dyestuffs, such as dyestuff **5**, which can enhance absorption at shorter wavelength regions. When dyestuff **5** was added to the dye solution, the IPCE of devices B and C at 350–500 nm increased significantly. The maximum IPCE increased from 35% to 65% when 0.25 molar ratio dyestuff **5** was added to the dye solution, and to 83% with 1 molar ratio dyestuff **5**. Upon dyestuff **5** co-adsorption, the maximum IPCE improved significantly, compared to that seen with device A, which can be attributed to the increased photocurrent of the DSSCs. The related experimental data are in line with the results in Table 2.

It is well known that organic dyestuffs will compete with N719 for the adsorption on the TiO_2 surface. As shown in Fig. 3 for devices B, and C and Table 2, there is a balanced relationship between the dyestuff **5** and N719 co-sensitizers. The IPCE spectra of device C shows a similar response at 570–800 nm, but broadens significantly at 350–570 nm in comparison with device A. This shows that N719 and dyestuff **5** are in balance at 1–0.25 molar ratio. In this concentration of co-sensitizers, N719 may occupy positions on the TiO_2 surface, as in device A, and dyestuff **5** then anchors to the blank to create a perfect insulating molecular layer. Because of this layer, the charge recombination process can be shielded, and the incident photo-to-electron conversion efficiency at shorter wavelengths can be enhanced, and this increases J_{sc} and η. On the other hand, device B shows a downward trend at 570–800 nm in comparison with device A, and the maximum IPCE is *ca.* 82% at 420 nm. This indicates that dyestuff **5** has considerable superiority at 1–1 molar ratio, with some N719 molecules having lost their positions on TiO_2 and being replaced by dyestuff **5**. This increases the opportunities for π–π stacking of organic dyestuff **5**, and decreases the contribution of N719 to the incident photon-to-electron conversion efficiency [20,21]. This is the reason why device B has lower conversion efficiency than device C in Table 2.

6. Conclusions

This study investigated the role of triazoloisoquinoline dyestuffs as co-adsorbents and co-sensitizers with N719. The results show that co-adsorption of N719 sensitizer with dyestuff **5** onto nanocrystalline TiO_2 films significantly increases the photocurrent in 1–0.25 molar ratio, thus enhancing the total conversion efficiency. The cell produced in this work achieved an energy conversion efficiency as high as 5.15% at 100 mW cm^{-2} and AM 1.5G. This improved conversion efficiency is attributed to the insulating molecular layer, which was composed of small molecule organic dyestuff **5** and N719, and the light harvesting effect at shorter-wavelength regions. It is anticipated that the findings of this work will contribute to the development of co-adsorbent and co-sensitizer bi-functional organic dyestuffs in DSSCs.

Acknowledgements

The authors thank the National Science Council of the Republic of China for financially supporting this research under Contract No. NSC 101-2113-M-011-002.

References

[1] B. O'Regan, M. Gratzel, Nature 353 (1991) 737.
[2] M. Gratzel, Nature 414 (2001) 338.
[3] M. Gratzel, J. Photochem. Photobiol. A 164 (2004) 3.
[4] P. Wang, C. Klein, R. Humphry-Baker, S.M. Zakeeruddin, M. Gratzel, J. Am. Chem. Soc. 127 (2005) 808.
[5] D.B. Kuang, P. Walter, F. Nüesch, S. Kim, J. Ko, P. Comte, S.M. Zakeeruddin, M.K. Nazeeruddin, M. Grätzel, Langmuir 23 (2007) 10906.
[6] J.H. Yum, S.R. Jang, P. Walter, T. Geiger, F. Nüesch, S. Kim, J. Ko, M. Grätzel, M.K. Nazeeruddin, Chem. Commun. (2007) 4680.
[7] J.N. Clifford, E. Palomares, Md K. Nazeeruddin, R. Thampi, M. Grätzel, J.R. Durrant, J. Am. Chem. Soc. 126 (2004) 5670.
[8] H. Choi, S. Kim, S.O. Kang, J. Ko, M.S. Kang, J.N. Clifford, A. Forneli, E. Palomares, M.K. Nazeeruddin, M. Grätzel, Angew. Chem. Int. Ed. 47 (2008) 8259.
[9] Q. Miao, L. Wu, J. Cui, M. Huang, T. Ma, Adv. Mater. 23 (2011) 2764.
[10] Y. Hong, J. Liao, D. Cao, X. Zang, D. Kuang, L. Wang, H. Meier, C. Su, J. Org. Chem. 76 (2011) 8015.
[11] V. Shrotriya, G. Li, Y. Yao, T. Moriarty, K. Emery, Y. Yang, Adv. Funct. Mater. 16 (2006) 2016.
[12] S. Roquet, A. Cravino, P. Leriche, O. Aleveque, P. Frere, J. Roncali, J. Am. Chem. Soc. 128 (2006) 3459.
[13] D. Kunag, S. Ito, B. Wenger, C. Klein, J.E. Moser, R. Humphry-Baker, S.M. Zakeeruddin, M. Gratzel, J. Am. Chem. Soc. 128 (2006) 4146.
[14] M. Liang, W. Xu, F. Cai, P. Chen, B. Peng, J. Chen, Z. Li, J. Phys. Chem. C 111 (2007) 4465.
[15] H. Tian, X. Yang, R. Chen, R. Zhang, A. Hagfeldt, L. Sun, J. Phys. Chem. C 112 (2008) 11023.
[16] B. Liu, W. Zhu, Q. Zhang, W. Wu, M. Xu, Z. Ning, Y. Xie, H. Tian, Chem. Commun. (2009) 1766.
[17] S. Ruhle, M. Greenstein, S.G. Chen, A. Merson, H. Pizem, C.S. Sukenik, D. Cahen, A. Zaban, J. Phys. Chem. B 109 (2005) 18907.
[18] J.H. Yum, P. Walter, S. Huber, D. Rentsch, T. Gieger, F. Nuesch, F.D. Angelis, M. Gratzel, M.K. Nazeeruddin, J. Am. Chem. Soc. 129 (2007) 10320.
[19] A. Mishra, N. Pootrakulchote, M.K.R. Fischer, C. Klein, M.K. Nazeeruddin, S.M. Zakeeruddin, P. Bauerle, M. Gratzel, Chem. Commun. (2009) 7146.
[20] X.F. Wang, H. Tamiaki, L. Wang, N. Tamai, O. Kitao, H. Zhou, S. Sasaki, Langmuir 26 (2010) 6320.
[21] F. Gao, Y. Cheng, Q. Yu, S. Liu, D. Shi, Y. Li, P. Wang, Inorg. Chem. 48 (2009) 2664.